

ON ESTIMATION OF EMPIRICAL ORTHOGONAL MODES IN INFLOW TURBULENCE FOR WIND TURBINES

K. Saranyasontorn and L. Manuel, M. ASCE

University of Texas, Austin, TX 78712

korn.ae@mail.utexas.edu, lmanuel@mail.utexas.edu

Abstract

An understanding of the inflow turbulence spatial structure is important in decisions related to siting of wind turbines. This study proposes the use of Proper Orthogonal Decomposition (POD) of the most energetic modes that characterize the spatial inflow random field describing the turbulence experienced by a wind turbine. The appeal for the use of POD techniques is that preferred spatial “modes” or patterns of wind excitation can be empirically developed using data from spatial arrays of sensed input/excitation. These loading modes explain in part the behavior of dynamic systems in an analogous way to how natural modes of vibration associated with response and developed using structure mass, stiffness, and damping properties can explain the same though again only in part. Proper orthogonal decomposition has generated much interest in wind engineering applications in recent years, albeit mainly for buildings, not for wind turbines. This study seeks to extend thinking related to this heuristically appealing approach to describing inflow by first examining the orthogonal subprocesses derived from a POD analysis defined by theoretical power spectra and coherence models commonly used for wind turbines. Then, based on field data from a wind turbine, estimates of cross-power spectral density functions are used to estimate empirical POD modes that are compared with those based on theoretical considerations. Accuracy in predicting power and coherence spectra from a limited number of POD modes is discussed.

Introduction

Proper Orthogonal Decomposition (POD) techniques have been employed in many applications to allow reduced-order representations of multivariate random fields. The eigenvectors from decomposition of cross-power spectral density (CPSD) matrices offer useful physical insights and identify spatially preferred patterns in each eigenmode. A feature of such spectral POD techniques is that, by truncation of higher eigenmodes associated with small eigenvalues, efficient computation schemes result that can describe the random field with accuracy. Recent studies by Carassale and Solari (2000) and Chen and Kareem (2003) have demonstrated the effectiveness of the POD approach in describing the coherence structure in wind turbulence random fields. Here we focus on implementing such techniques to characterize the inflow that influences a horizontal-axis wind turbine. In wind turbine applications, there has been limited use of POD techniques. An initial study on the turbulence modeling of the wind turbine inflow environment using POD was recently carried out by Spitler et al (2004) where the eigenmodes were computed by decomposing the covariance matrix of a discrete zero-mean, stationary random process. Here, our focus is on a spectral POD approach that employs CPSD matrices describing the inflow over a range of frequencies. We first study POD modes derived based on theoretical power spectra and coherence models typically used in wind turbine design (IEC, 1998). Then, turbulence field data are employed in deriving empirical orthogonal modes. Theoretical and estimated orthogonal modes are compared and the accuracy of reduced-order representations using a limited number of POD modes of power spectra at various frequencies and of coherence functions is assessed for different spatial separations.

Spectral Proper Orthogonal Decomposition

Let $\mathbf{V}(t) = \{V_1(t), V_2(t) \dots V_N(t)\}^T$ be a zero-mean, weakly stationary Gaussian vector random process describing the along-wind inflow turbulence at N spatial locations, $\mathbf{x}_1, \mathbf{x}_2, \dots, \mathbf{x}_N$, such that $V_i(t) = V(\mathbf{x}_i, t)$ where $\mathbf{x}_i = (x_i, y_i, z_i)$. Second-moment statistics between any two processes, $V_i(t)$ and $V_j(t)$, can be expressed in terms of the CPSD matrix, $\mathbf{S}_V(f)$ that contains terms such as $S_V^j(\mathbf{x}_i, \mathbf{x}_j, f)$, at any frequency, f . The process, $\mathbf{V}(t)$ can be decomposed into N orthogonal subprocesses, $\mathbf{W}_n(t)$, where $n=1,2,\dots,N$, as follows

$$\mathbf{V}(t) = \sum_{n=1}^N \mathbf{W}_n(t). \quad (1)$$

Each of these subprocesses is obtained following solution of the eigenvalue problem,

$$\mathbf{S}_V(f)\Phi(f) = \Lambda(f)\Phi(f) \quad (2)$$

where $\Phi(f) = \{\phi_1(f), \phi_2(f) \dots \phi_N(f)\}$ and $\Lambda(f) = \text{diag}\{\lambda_1(f), \lambda_2(f) \dots \lambda_N(f)\}$ are eigenvectors and eigenvalues of the $N \times N$ CPSD matrix, $\mathbf{S}_V(f)$. Since $\mathbf{S}_V(f)$ is Hermitian, the eigenvalues are real and positive. Further, if all components in the CPSD matrix are real, the eigenvectors are also real. If the spectral eigenvalues, $\lambda_n(f)$, are arranged in decreasing order, a reduced-order POD representation of $\mathbf{S}_V(f)$ may be obtained by retaining only the first N_s orthogonal eigenmodes (where $N_s \leq N$):

$$\hat{\mathbf{S}}_V(f) = \sum_{n=1}^{N_s} \lambda_n(f) \phi_n(f) \phi_n^*(f) \quad (3)$$

where the asterisk is used to denote the conjugate and transpose operator. Note that, at any frequency, diagonal terms in $\hat{\mathbf{S}}_V(f)$ represent PSD estimates from N_s subprocesses while off-diagonal terms are related to coherence function estimates at various separations (according to the locations, $\mathbf{x}_1, \mathbf{x}_2, \dots, \mathbf{x}_N$). An attractive feature of the POD technique is that the reduced-order POD representation of $\mathbf{S}_V(f)$ is optimal compared to any other linear orthogonal decomposition.

Numerical Examples

Part I: POD and Spectral Models for Inflow Turbulence for Wind Turbines

The effectiveness of the use of reduced-order POD modes derived from turbulence spectral models recommended in the IEC guidelines (IEC, 1998) for inflow simulation for wind turbine design is studied. Consider a turbine with a rotor plane of radius 8.5 meters and a hub height of 23 meters. To carry out the POD analyses, the rotor plane is discretized so as to yield 49 nodal points as shown in Fig. 1. The CPSD matrix, $S_V^j(\mathbf{x}_i, \mathbf{x}_j, f)$, that describes the spectral character of the inflow turbulence over the rotor plane is assumed to be given by the Kaimal spectral model (Kaimal, 1972),

$$\frac{f \cdot S_V(\mathbf{x}_i, \mathbf{x}_j, f)}{u_*^2} = \frac{A(fz/U)}{[1 + B(fz/U)]^{5/3}} \quad (4)$$

and an exponential coherence model (Davenport, 1961) which yields

$$S_V^2(\mathbf{x}_i, \mathbf{x}_j, f) = \exp[-c(fr/U)] \cdot S_V(\mathbf{x}_i, \mathbf{x}_i, f) \cdot S_V(\mathbf{x}_j, \mathbf{x}_j, f) \quad (5)$$

where z is the elevation under consideration and the parameters A , B , and c are 105, 33, and 15.4, respectively, for the along-wind turbulence component whose mean value over

ten minutes is U . Also, the shear velocity, u_* , is $0.4U/\ln(z/z_0)$ where z_0 is the surface roughness taken to be 0.5 cm here. The CPSD matrix may be constructed using Eqs. (4) and (5), and then decomposed into spectral proper orthogonal modes. Figure 2 shows the eigenvalues, $\lambda_n(f)$, for several different eigenmodes. Especially in the low-frequency region, the first mode eigenvalue is significantly higher than the other eigenvalues. At higher frequencies, this is not so and greater truncation of modes may only be possible at low frequencies. The first six spectral eigenvectors, $\phi_n(f)$ ($n = 1$ to 6), at a frequency of 0.1 Hz are shown in Fig. 3. The corresponding eigenvalues for each mode are also shown. It is seen that the first mode describes a mostly uniform spatial inflow structure over the rotor plane while the second and third modes (with similar energy levels) describe spatial shear of the inflow turbulence in the vertical (z) and lateral (y) directions, respectively. As expected, the higher eigenmodes have more complex spatial patterns.

Next we attempt reconstruction of power spectral densities by employing a subset of the proper orthogonal modes. Figure 4 shows PSD reconstruction using 1, 3, 6, 15, and 30 modes at the top and center of the rotor. As expected, a very small number of modes are needed to accurately describe low-frequency inflow energy while a much larger number is required at higher frequencies. It can also be noticed that reconstruction is more efficient at the center of the rotor than at the top. Finally, we study coherence as described by using a subset of the orthogonal modes. Figure 5 shows coherence spectra reconstructed using 3, 6, 15, and 30 modes for four different separations (2.83, 5.67, 8.50, and 17.0 meters) that result from considering nodal location pairs (1,6), (1,22), (1,38), and (38,46), respectively, as identified in Fig. 1. It is seen that the first six modes might be sufficient to describe coherence over separations of 8.5 meters or greater. Over shorter separations, especially at higher frequencies, additional modes may be necessary.

Part II: POD and Estimates of Cross-Power Spectral Density Functions from Field Data

Field measurements including structural response/loads at a wind turbine and inflow turbulence data upwind of the turbine were recorded as part of the Long-Term Inflow and Structural Test (LIST) program carried out by Sandia National Laboratories at a site in Bushland, Texas in 2000 (Sutherland et al, 2001). Here, we discuss how the turbulence data might be used to empirically estimate spectral proper orthogonal modes. Comparisons of the derived modes with those found in Part I are discussed as are estimates of power spectra and coherence based on a limited number of modes. An illustration of the test turbine and spatial array that included only five sonic anemometers over the rotor plane is shown in Fig. 6. Only the along-wind component of turbulence recorded by the three-component anemometers is considered here. In order to estimate the five POD modes, a CPSD matrix was first estimated by fitting the Kaimal spectral model (Kaimal, 1972) and the Davenport coherence (Davenport, 1961) model to data. Based on least-squares fits, the parameters, A , B , and c , in Eqs. (4) and (5) were estimated to be 124, 37, and 21, respectively. Eigenvalues and eigenvectors were computed using the estimated CPSD matrix. For the sake of illustration, the first three eigenmodes and corresponding eigenvalues at a frequency of 0.1 Hz are presented in Fig. 7. As we saw in Fig. 3, the first mode describes an almost uniform inflow spatial pattern over the rotor plane while the second and the third modes describe sheared shapes again similar to those seen in Fig. 3. The first eigenvalue based on the field data is not as dominant over the

next two eigenvalues as was seen in Fig. 3. Also, employing real field data does not preserve all of the symmetry that we saw in Part I and, as a result, modes 2 and 3 do not have identical eigenvalues.

Using the first three POD modes, example PSDs and coherence functions are estimated and compared with (target) spectra obtained from data in Figs 8 and 9, respectively. Figure 8 shows reconstruction of the PSD at the top and center of the rotor. While these three modes are sufficient to describe the PSD at the center of the rotor at almost all frequencies, they are insufficient for the top of rotor at high frequencies. Figure 9 shows that coherence spectra based on three modes are reasonably accurate over the longest separations studied for the rotor plane (17 meters) but grossly inaccurate at shorter separations suggesting the need for additional modes over small separations.

Conclusions

It has been demonstrated that the spectral character of inflow turbulence that affects wind turbines might be studied by examining the proper orthogonal modes derived from cross-power spectral density (CPSD) functions. In this paper, we showed how standard PSD and coherence models in use for wind turbine design can yield all the orthogonal modes but a subset of these can describe the overall random field with varying degrees of accuracy – especially at high frequencies, a greater number of modes are required for describing the PSD. Coherence, similarly, is not well predicted over short separations using a small subset of orthogonal modes. Field data were employed to assess empirical modes with similar results as when standard spectral models were employed.

Acknowledgements

The authors acknowledge financial support provided by Grant No. 003658-0272-2001 through the Advanced Research Program of the Texas Higher Education Coordinating Board and by Grant No. 30914 from Sandia National Laboratories. They are also grateful to Dr. Herbert J. Sutherland for providing the field data from the LIST program.

References

- Carassale, L. and G. Solari, (2000), "Proper Orthogonal Decomposition of Multi-Variate Loading Processes," Proc. 8th ASCE Specialty Conf. on Prob. Mech. and Structural Reliability, PMC2000-282.
- Chen, X. and A. Kareem, "POD in reduced order modeling of dynamic load effects," Proc. Ninth Intl. Conf. on Applications of Statistics and Probability in Civil Engrg. (ICASP9), San Francisco, July 2003.
- Davenport, A. G., "The Spectrum of Horizontal Gustiness near the Ground in High Winds," Quarterly Journal of the Royal Meteorological Society, Vol. 87, pp. 194-211, 1961.
- IEC, "Wind Turbine Generator Systems Part 1: Safety Requirements," International Electrotechnical Commission (IEC), IEC/TC 88 61400-1, Ed. 2, 1998
- Spitler, J. E., S. A. Morton, J. W. Naughton, and W. R. Lindberg, "Initial Studies of Low-Order Turbulence Modeling of the Wind Turbine In-flow Environment," Proceedings of the ASME Wind Energy Symposium, AIAA-2004-1004, January 2004.
- Sutherland, H. J., P. L. Jones, and B. A. Neal, "The Long-Term Inflow and Structural Test Program," Proceedings of the ASME Wind Energy Symposium, AIAA-2001-0039, January 2001.
- Kaimal, J. C., J. C. Wyngaard, Y. Izumi, and O. R. Cote, "Spectral Characteristics of Surface Layer Turbulence," Quarterly Journal of the Royal Meteorological Society, Vol. 98, pp. 563-598, 1972.

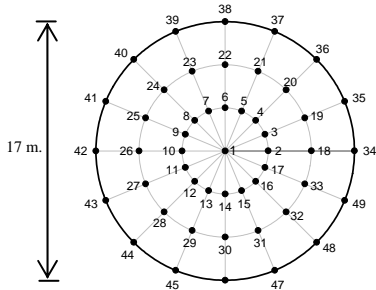


Figure 1: Forty-nine spatial locations of points used in POD analyses. (Point 1 is at center of rotor plane.)

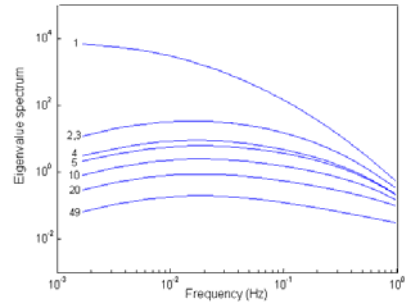


Figure 2: Eigenvalues as a function of frequency for different POD modes.

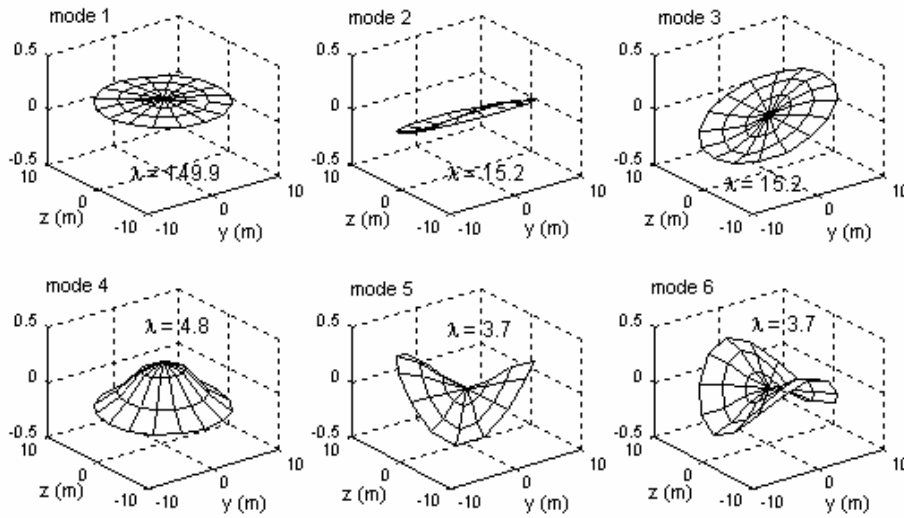


Figure 3: First six eigenmodes at 0.1 Hz and the corresponding eigenvalues.

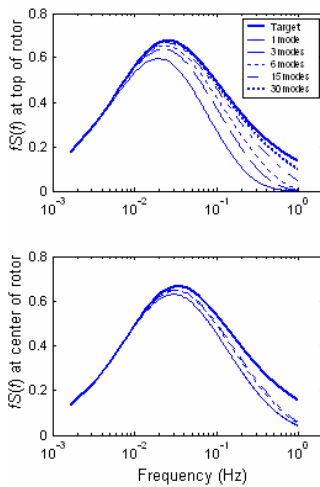


Figure 4: Reconstruction of PSDs at two different locations.

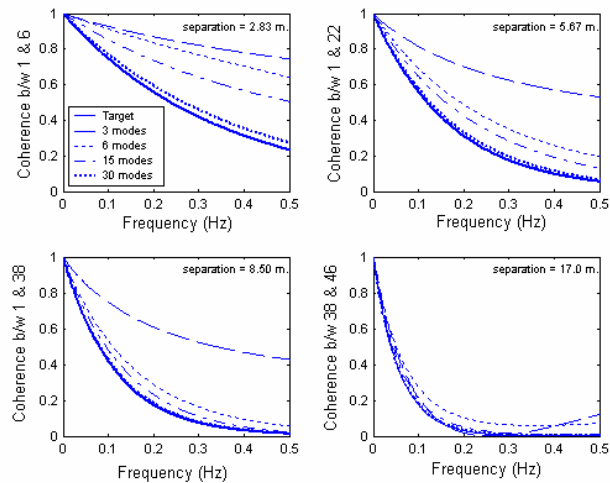
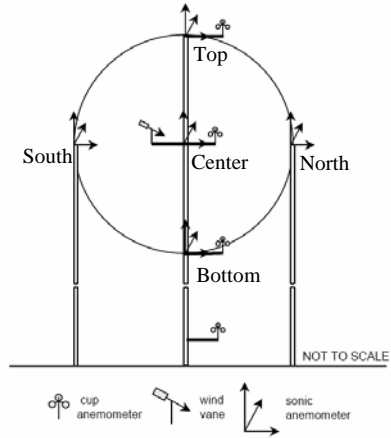


Figure 5: Reconstruction of coherence functions at four different separations.



(a)



(b)

Figure 6: (a) The LIST wind turbine and (b) the primary inflow instrumentation on towers upwind of the turbine.

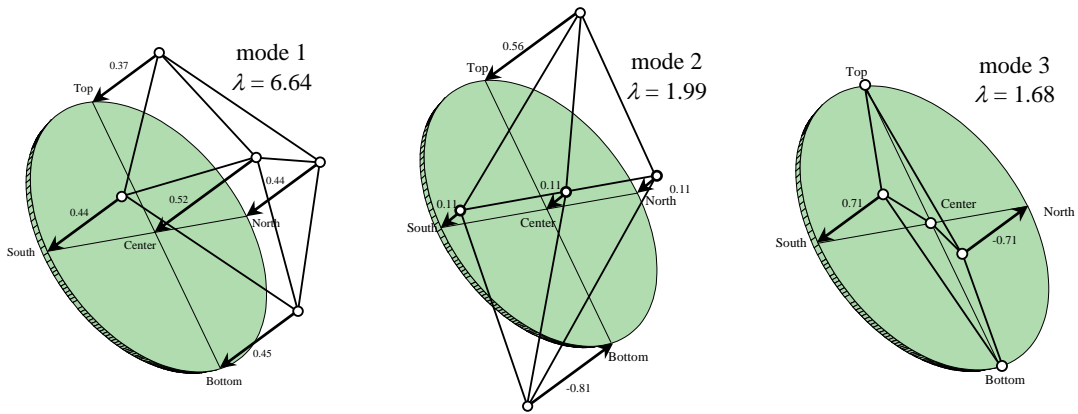


Figure 7: First three eigenmodes at 0.1 Hz and corresponding eigenvalues based on field data.

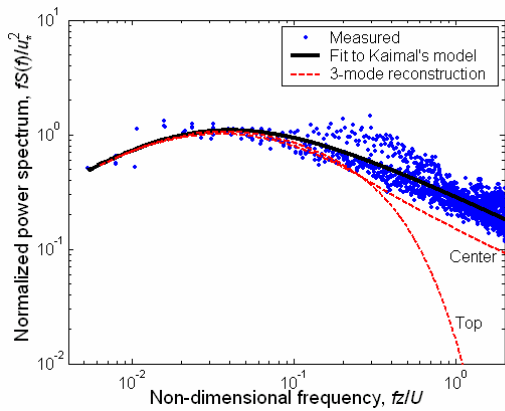


Figure 8: Estimated normalized PSDs for along-wind turbulence at center and top of rotor, Kaimal model fit, and PSD reconstruction using 3 modes.

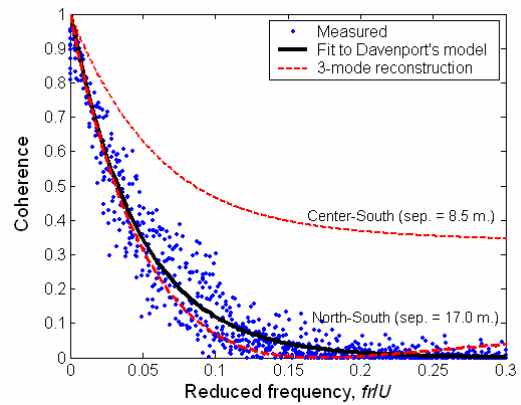


Figure 9: Estimated coherence functions for along-wind turbulence at two separations, Davenport model fit, and coherence function reconstructions using 3 modes.